Scrutinizing Evaporation Models for Computational Modelling of Turbulent Sprays

D. Kolaitis and M. Founti*

Laboratory of Heterogeneous Mixtures and Combustion Systems, Thermal Engineering Section, Mechanical Engineering Department, National Technical University of Athens, Heroon Polytechniou 9, Polytechnioupoli Zografou, 15780 Athens, Greece.
Tel. +30-210-7723605, Fax. +30-210-7723663
*Corresponding author e-mail: mfou@central.ntua.gr

One of the major phenomena influencing the operational characteristics of conventional liquid fuel combustion systems is droplet evaporation. In order to determine the best available droplet evaporation model for implementation in a two-phase CFD code, three such models are compared and evaluated, following a two-stage procedure. Initially, the predictive capability as well as the numerical efficiency of each model is assessed for the case of a single, evaporating droplet, positioned in a convective environment. Then all models are implemented in a two-phase CFD code and their physical and computational behaviour is evaluated for the case of a fully turbulent evaporating spray., Numerical predictions obtained with each model are validated with available experimental data for both test cases. The model of choice is a non-equilibrium droplet evaporation model, which yields results that agree reasonably well with measurements, while at the same time has a relatively low computational cost.

Topics: Theory and implementation of spray modelling, Spray combustion, Droplet evaporation

1. Introduction

Among the wide spectrum of industrial applications of spray technologies (e.g. spray drying, coating, hydrophibization, water-jet cutting), combustion processes are the most delicate to control and optimize, involving simultaneous momentum-mass-energy transfer and chemical reactions. Oil fired furnaces and boilers, diesel engines and gas turbines utilize liquid fuel sprays with the aim of increasing the fuel surface area and thus accelerating the vaporization and combustion rates. Conventional liquid fuel burning technologies, inject the fuel into the combustion chamber through a nozzle that atomises it, producing a spray comprising many droplets, typically the order of a few tens to a few hundreds of microns in diameter. The droplets, subjected to the high temperatures of the combustion chamber, are evaporated and burnt in a partially sequential process. Towards the scope of computationally simulating the complete combustion process, there arises a need to model effectively the phenomena involved in droplet evaporation.
The purpose of the present work is to evaluate a number of droplet evaporation models, available in the literature, for low-pressure, stochastic spray computational fluid dynamics (CFD) simulations. The comparison and evaluation of three evaporation models is performed in two stages. At first, the ability of the evaporation models under consideration to accurately

describe the temporal evolution of both diameter and temperature of single isolated droplets, evaporating in a constant temperature and constant velocity air environment is assessed by comparison with relevant experiments. As a result, the most promising model is established in terms of both physical accuracy and numerical efficiency. In a second stage, a confined evaporating turbulent spray test case is considered and an in-house two-phase Eulerian-Lagrangian CFD code is used in order to simulate the spray evolution. Predictions of spray evaporation characteristics obtained with each model are compared with available experimental data and the applicability and performance of each model for implementation in a CFD code is evaluated.

2. Droplet evaporation models

The evaporation models examined span the history of evolution of droplet evaporation modelling. At first, the "standard" d^2-law Spalding model [1] is considered in a slightly different form than the original, proposed by Spalding on 1953. An energy equation is introduced, assuming an infinite thermal conductivity for the liquid. The second model considered is the one proposed by Abramzon and Sirignano [2]. The model, which incorporates the effects of Stefan flow on heat and mass transfer, has started attracting attention during the last decade and has already been implemented in numerous commercial and non-commercial CFD codes. Then, the Bellan and Harstad non-equilibrium model [3] is examined, based on the Langmuir-Knudsen law. This model, while quite promising, is relatively new and has not yet been tested and implemented in CFD codes, contrary to the ones previously mentioned. Finally, a "modified" form of the "standard" Spalding model is investigated.

2.1. "Standard" Evaporation Model (EM1)

In 1953 [1], Spalding suggested that the mass evaporation rate $\dot{m}$ (kg/s) of a single, isolated droplet, evaporating in an infinite, constant temperature and constant velocity air environment, should be computed by using the following equation:

$$\dot{m} = \pi D_p \rho_m D_{AB} Sh \ln(1+B_M) \tag{1}$$

where B_M is Spalding's non-dimensional mass transfer number. The surface equilibrium mole fraction of the fuel vapour is calculated utilizing the Clausius-Clapeyron equilibrium vapour pressure equation. Historically, the Spalding model was developed assuming a constant droplet temperature, fixed at the wet-bulb condition. Since then, it has been recognized that the transient droplet heating phenomena have a quite significant effect on the evaporation process. As a result, the "classic" evaporation rate equation is coupled with a time-dependent energy equation, making use of the infinite liquid conductivity hypothesis, which assumes that the droplet has a uniform, but time-varying temperature. This procedure correctly represents the fact that a droplet within a spray has no fixed wet-bulb temperature due to the continuous change in the properties of its surroundings [4]. The heat balance equation for the droplet is written in the following form:

$$m_p C_{p,l} \frac{dT_p}{dt} = \pi D_p Nuk_m \left(T_\infty - T_p\right) - \dot{m}L \tag{2}$$

2.2. "Stefan Flow" Evaporation Model (EM2)

Abramzon and Sirignano revised the infinite conductivity model to incorporate the effects of Stefan flow on heat and mass transfer [2]. They introduced two correction factors, namely F_T and F_M, which represent the relative change of the thermal and diffusional film thicknesses due to the Stefan flow, in order to take into consideration the fact that surface blowing results in the thickening of the thermal and mass boundary layers. In this case, the droplet's mass evaporation rate is calculated using Equation (1), by substituting the Sherwood number with its modified value (Sh*). The droplet's energy equation is cast in the following form:

$$m_p C_{p,l} \frac{dT_p}{dt} = \dot{m}\left(\frac{C_{p,vap}\left(T_\infty - T_p\right)}{B_T} - L \right) \tag{3}$$

where B_T is Spalding's non-dimensional heat transfer number. Here, the Nusselt number is substituted by its modified value (Nu*). It should be noted that in this case, the calculation of the mass evaporation rate ($\dot{m}$) as well as the droplet's surface temperature (T_p) is not as straightforward as in the previous case, since here there is a need for an iterative procedure so as to calculate the value of Spalding's heat transfer number (B_T).

2.3. "Non-Equilibrium" Evaporation Model (EM3)

Bellan and Harstad proposed an evaporation model which takes into consideration the non-equilibrium phenomena that may appear in the gas-droplet interface [5]. Their original model, based on the Langmuir-Knudsen law, incorporated also a finite liquid conductivity model, which assumed a non-uniform temperature profile across the droplet radius. Since there are references in the literature proposing that there are no significant improvements observed by the implementation of the finite conduction model compared to the infinite conductivity model [6], the latter one was chosen to be used in the model under consideration. The non-equilibrium Langmuir-Knudsen law was incorporated through the definition of a non-equilibrium vapour mole fraction at the droplet surface [3]:

$$\chi_{F,s,neq} = \chi_{F,s} - (2\, L_K\, \beta / D_p) \tag{4}$$

where L_K represents the Knudsen layer thickness, while the non-dimensional evaporation parameter β is given by:

$$\beta = \frac{Cp_G \dot{m}}{2\pi k_G D_p} \tag{5}$$

Mass transfer at the surface of the droplet tends to reduce the Nusselt number, since the streaming vapour leaving the surface must be heated in the boundary layer until it reaches the ambient temperature at the edge of it. The energy absorbed by this superheating process is being subtracted from the potential energy that can reach the liquid surface. A further reduction in the Nusselt number value is attributed mainly to the increase of boundary layer thickness due to the surface blowing. In order to take account of the aforementioned phenomena, a Nusselt number correction is introduced:

$$Nu^{*} = Nu_0\left(\frac{\beta}{e^{\beta}-1}\right) \tag{6}$$

In this case, the droplet heat balance equation used is Equation (2), where the Nusselt number is substituted by the modified Nu^{*}.

2.4. Convective heat and mass transfer correlations

Due to the fact that the droplet has a non-zero slip velocity with respect to the air stream, which is surrounding it, the gas-phase mass boundary layer is exposed to a convective environment. Gas-phase convection influences the droplet vaporization process in a two-fold manner: not only does it increase the gasification rate as well as the heat transfer rate between the phases, but it also generates liquid circulation inside the droplet with consequent increase of the liquid-transfer rate. In order to account for these phenomena, the diffusive mass flux and energy transfer expressions are multiplied by the droplet Sherwood and Nusselt numbers, respectively, corrected semi-empirically for the case of forced convection.
There is a variety of semi-empirical correlations available in the literature, for the convective correction of both mass and heat transfer equations. Nevertheless, for moderate evaporation rates, no significant differences have been observed among predictions utilizing various correlations [7]. Thus, the well-known Ranz and Marshall correlations [8] are used. Finally, the fuel vapour and the gas phase species properties at the "film" surrounding the droplet are determined using the well-known "1/3-rule", the standard additive rules for ideal gas and the Wilke mixing rule.

3. Model comparison for a single evaporating droplet

The three evaporation models under consideration are compared and evaluated against experimental data for a single-component fuel droplet evaporating in a forced convection environment. The time dependent droplet diameter and temperature predictions are compared to the experiments of Wong and Lin [9], where a decane droplet of initial diameter $D_{p,0}$=2.0mm and temperature $T_{p,0}$=315K is suspended against a constant velocity (u_{∞}=0.698m/s) and temperature (T_{∞}=1000K) air stream. The air temperature is much higher than the droplet's boiling point (T_{BP}=447.7K) therefore vigorous evaporation rates can be expected.
An overall comparison between experimental data and computational predictions for the temporal evolution of the droplet's squared diameter and temperature is presented in Figure 1. The relatively large temperature difference between the droplet and its surrounding airstream results in a strong initial heat-up stage during which the well-known d^2-law is invalid. The combination of this prolonged heat up period with the observed high evaporation rate results in some discernible discrepancies between the various model predictions for both the droplet diameter and temperature values. A general observation is that predictions of models EM1 and EM2 lie on either side of the experimental data, not being able to follow them closely. EM3 predictions agree reasonably well with experiments.
It is evident that EM1 (Figure 1) overpredicts the droplet temperature, resulting in higher evaporation rate and consequently shorter evaporation time than the respective measured values. On the other hand, EM2 temperature predictions are lower than the experimental values resulting to total evaporation time larger than the measured one.

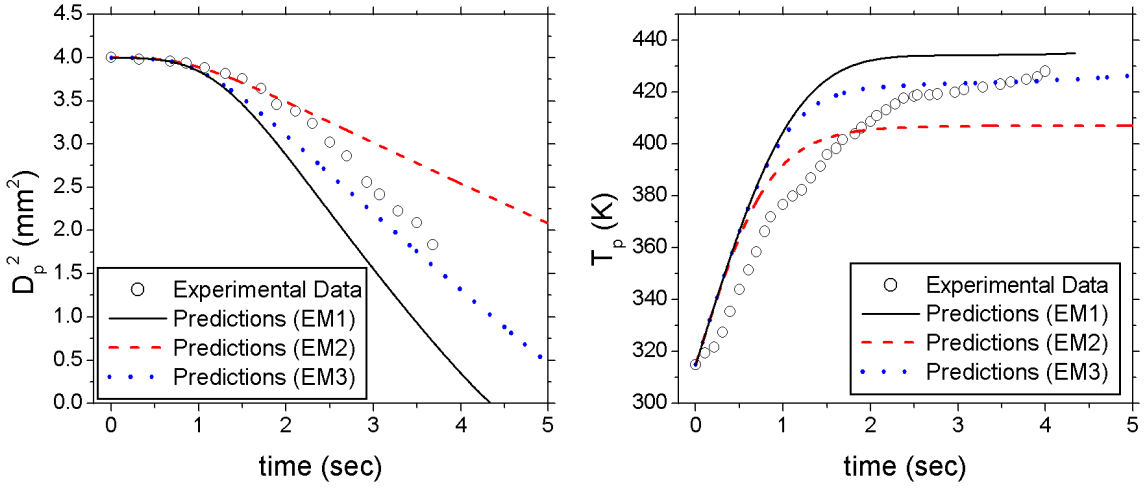

Figure 1 Temporal evolution of a decane droplet's squared diameter and temperature, evaporating in a heated airstream.

Only EM3 droplet temperature predictions lie closest to the experimental values, despite the discrepancies observed during the initial heat-up period. This remark suggests that the heat transfer modification introduced in EM3, see equation (6), outperforms the respective "blowing effect" correction factors introduced in EM2. Overall, for a high evaporation rate environment, EM1 and EM2 exhibit a rather poor performance, while EM3 yields reasonable results regarding both droplet diameter and temperature predictions, rendering it the model of choice for implementation into a CFD code.

The aforementioned conclusion is further supported by the relative CPU-time requirements among the examined models, presented in Table 1. The actual CPU-times are "normalized" using the respective value of EM1 as reference. It is evident that EM1 and EM3 are computationally less expensive compared to EM2. The sophisticated and numerically complex iterative procedure needed by EM2 to calculate the heat mass transfer correction term, introduces a large CPU burden on the modelling effort, thus resulting in excessive CPU-time requirements (more than double in comparison to the other two models). On the contrary, despite the fact that EM3 exhibits comparatively the best predictive capabilities, it only requires approximately 9% more CPU-time than EM1.

Table 1 Droplet evaporation models CPU-time requirements

Test Case	Single Droplet	Evaporating Spray
EM1	100.0 %	100.0 %
EM2	240.1 %	139.8 %
EM3	108.8 %	106.5 %

4. Model comparison for a turbulent evaporating spray

In order to evaluate each model's ability to accurately predict the nature of the heat and mass transport phenomena involved in a spray, as well as their numerical stability and robustness, all three models are implemented in a two-phase CFD code. The CFD code used to model the two-phase flowfield is a modified version of the 2PHASE code developed in the Laboratory of Heterogeneous Mixtures and Combustion Systems of NTUA. The code is based on the

Eulerian-Lagrangian computational formulation for the continuous and dispersed phases respectively and has been previously validated in a variety of diverse two-phase flow cases [10-12] yielding satisfactory predictions compared to experimental data.

The continuous phase is treated as a steady, incompressible and turbulent flow and is computed by solving the time-averaged continuity, species concentration, momentum and energy transfer equations. The resulting system of equations is solved via a finite volume method based on a staggered grid arrangement, using the SIMPLE [13] algorithm and a hybrid differencing discretization scheme. Turbulence quantities are modelled using a modified version of the k-ε turbulence model [14], which modifies the constants C_μ and C_2 of the standard k-ε model to account for the radius of curvature of the flow. This model has proved to yield better prediction accuracy than the standard k-ε model in recirculating flows with abrupt area changes [12].

Lagrangian treatment is adopted for the dispersed phase, where a large number of droplet "parcels" representing a number of real droplets with the same properties are traced through the flowfield. Each parcel's trajectory is calculated by solving the instantaneous droplet momentum and energy equations in a three-dimensional Cartesian frame of coordinates, with the use of a 4^{th} order Runge-Kutta method. The particle motion equations take account of the drag force, the lift force due to particle rotation, the pressure gradient force, the shear lift force and the gravitational force. The droplet turbulent dispersion is modelled by sampling random Gaussian gas velocity fluctuations and accounting for the crossing trajectories and eddy life time effects [15]. The gas and the liquid phase are coupled by calculating source-sink terms for the interfacial mass, momentum, species concentration, thermal and turbulent energy exchange (two-way coupling), following a modified version of the PSI-cell approach [16]. In order to improve the accuracy of the droplet massflow rate predictions near the symmetry axis, a "drift correction" term is applied to the turbulent dispersion model, across the transverse direction [17].

Velocity and particle size measurements at a hollow-cone spray [18] have been used to validate the model performance. For the experiments, isopropyl alcohol with a temperature of 313K, was injected downwards to a 194mm inner diameter cylindrical test section, utilizing a 20mm outer diameter SIMPLEX nozzle positioned at the pipe's symmetry axis. The co-flowing air stream, preheated at 373K, was simultaneously blown through a concentric annulus with an outer diameter of 64mm. Detailed experimental radial profile measurements at various axial positions were provided for validating the numerical predictions, whereas the first radial profile at x=3mm has been used to set the initial conditions for the CFD simulation. The inlet mass flow rates of air and isopropyl alcohol were measured to be 28.3g/s and 0.443g/s respectively, thus rendering the spray as a very dilute two-phase flow.

The computational domain, measuring 1.0m axially by 0.1m radially, was discretized using 131*70 non-uniform, cylindrically axisymmetric, rectangular grid nodes. The grid was refined close to the nozzle tip to improve local flow resolution. This grid arrangement yielded similar results to those obtained by using a grid with 183*125 nodes, thus ensuring grid independence. The droplets were considered to be spherical and were launched from 10 discrete starting locations along the nozzle. A total number of 30 000 droplet "parcels" was injected and tracked throughout the flow-field, for 30 two-way coupling iteration cycles.

In Figure 2, computational predictions for the radial distribution of the main droplet characteristic quantities (namely mean axial velocity, mean Sauter diameter and liquid mass flux), utilizing all three evaporation models under consideration, are compared to available experimental data, for various axial downstream positions. It is apparent that all models yield reasonably accurate results. Predictions for both droplet mean axial velocity and liquid massflux are insensitive to the specific evaporation model used, whereas for the droplet mean

Sauter diameter there is only a marginal sensitivity observed, especially at radial positions near the outer spray edge. These remarks are consistent with similar observations in the literature [19]. Only minor discrepancies are observed among the various model predictions, thus indicating that in the low evaporation rate conditions of the examined turbulent spray test case, all models perform equally well, "masking" the previously observed advantages of EM3. There is a general lack of experimental data for high evaporating rate sprays that could be used to demonstrate the specific predictive capabilities of the three different models.

As can be seen in Figure 2a, droplet mean axial velocities become more uniform with increasing distance from the nozzle since large droplets, having initially higher slip velocities, decelerate more rapidly than small droplets due to the non-linear nature of the drag law. Computational predictions lie quite close to the experimental data, except from some radial positions very close to the symmetry axis. A similar behaviour may be also observed in the liquid massflux predictions presented in Figure 2c and is mainly attributed to the well-known issue of unrealistic accumulation of droplet mass fluxes near the spray centreline, which has been partially remedied by the implementation of a drift-correction term in the droplet turbulent dispersion model [17, 19]. A typical hollow cone Simplex-spray spatial evolution history emerges in Figure 2b, i.e. the droplet mean Sauter diameter is generally increasing with the radial distance from the central axis. Also in this case, all models perform reasonably well, apart from some discrepancies observed near the spray's edge.

All in all, it is evident that an overall satisfactory quantitative agreement is achieved between the experimental measurements and the numerical predictions with all the examined evaporation models, thus revealing insignificant differences in their predictive capabilities. Nevertheless, by looking at the respective CPU-time usage comparison in Table 1, it becomes apparent that once more, EM2 exhibits higher CPU-time requirements in comparison to the other models (although in this case, the "excessive" time needed is decreased, ranging from 33% to 40% as compared to EM3 and EM1 respectively). Therefore, the conclusions of the previous analysis in relation to the single droplet evaporation modelling are further corroborated, towards the selection of EM3.

5. Conclusions

Three droplet evaporation models, namely the Spalding model (EM1), the Abramzon and Sirignano model (EM2) and the Bellan and Harstad model (EM3) have been compared and evaluated against existing experimental data for two different test cases. The first case pertained to a single droplet evaporating in a convective environment, exhibiting high evaporation rate conditions, while the second case referred to a fully turbulent, atmospheric pressure, evaporating spray, which has been numerically simulated using a two-phase Eulerian-Lagrangian CFD code. The implementation of EM3 resulted to a significant improvement over EM1 and EM2 in predicting both droplet diameter and temperature lifetime histories in the single droplet, high evaporation rate condition, whereas all models demonstrated similar behaviour in the frame of the mild evaporation rate, turbulent spray. These findings, supported by the CPU-time consumption comparison which revealed that EM3 inflicts a relatively modest computational effort to the modelling procedure (which is slightly higher in respect to EM1 but extremely lower when compared to EM2), suggest that the most promising droplet evaporation model, capable of dealing successfully with a variety of evaporating conditions, while not introducing a large CPU burden on the computational procedure, is the non-equilibrium model of Bellan and Harstad (EM3).

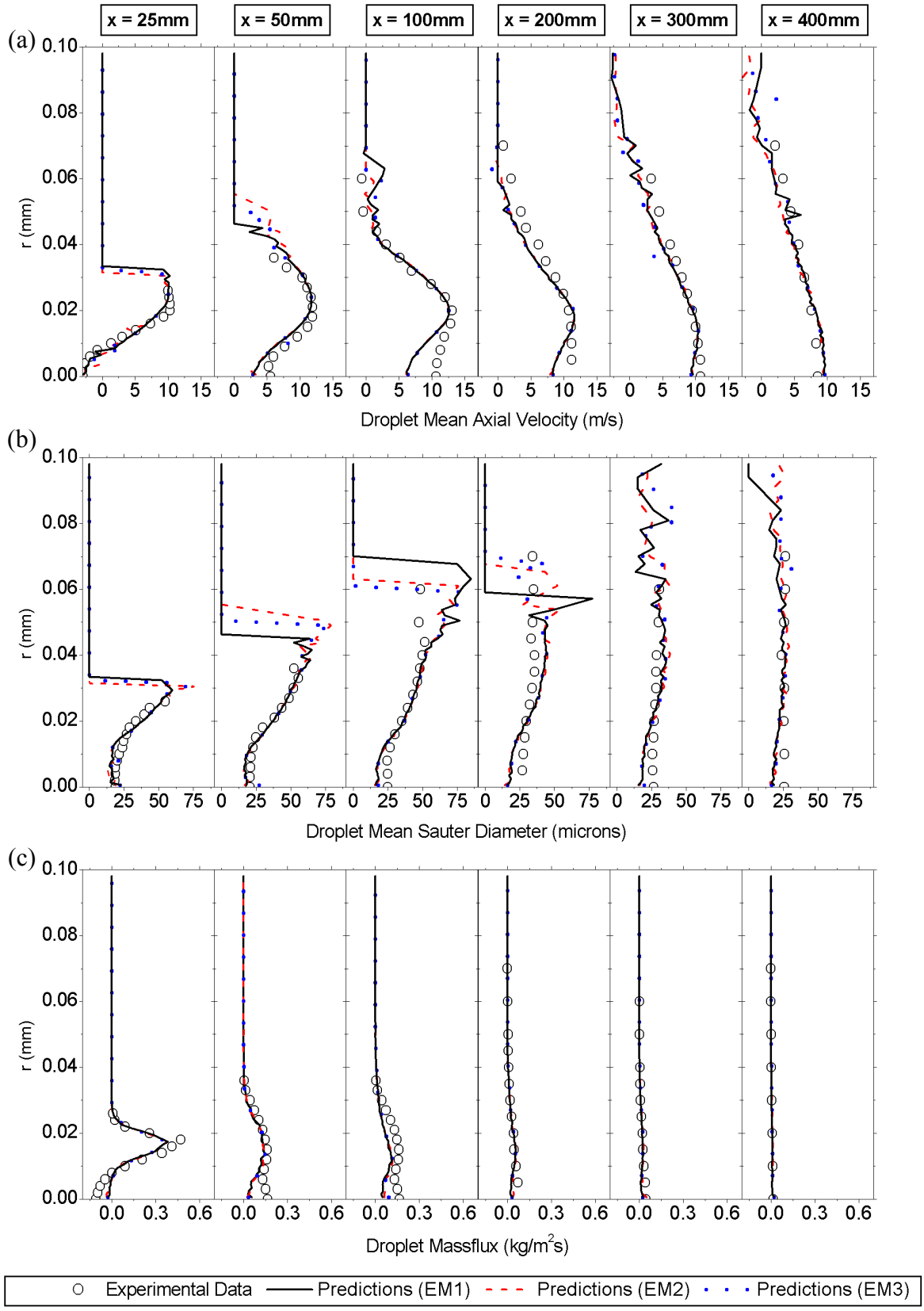

Figure 2 Comparison of measured and computed radial profiles for (a) droplet axial mean velocity, (b) droplet mean diameter and (c) droplet liquid massflux

6. References

[1] Spalding D B 1953 *Proc. 4th Symp. (International) on Combustion* 847-864
[2] Abramzon B and SirignanoW A 1989 *Int. J. Heat Mass Transfer* **32** 1605-1618
[3] Miller R S, Harstad K and Bellan J 1998 *Int. J. of Multiphase Flow* **24** 1025-1055
[4] Faeth G M 1983 Prog. Energy Combust. Sci. **9** 1-76
[5] Bellan J and Harstad K 1987 Int. J. Heat Mass Transfer **30** 125-136
[6] Berlemont A, Grancher M S and Gouesbet G. 1991 *Int. J. Heat Mass Tran.* **34** 2805-2812
[7] Kolaitis D and Founti M 2002 *Proc. 10th Workshop on Two-Phase Flow Predict.* 72-81
[8] Ranz W E and Marshall W R 1952 *Chem. Engng. Prog.* **48** 141-146
[9] Wong S C and Lin A R 1992 *J. Fluid Mech.* **237** 671-687
[10] Kolaitis D I and Founti M A 2002 *Proc. 18th ILASS Europe* 415-420
[11] Klipfel A, Founti M, Zaehringer K., Martin J P and Petit J P 1998 *Flow, Turb. Comb.* **60** 283-300
[12] Founti M and Klipfel A 1998 *Experimental Thermal and Fluid Science* **17** 27-36
[13] Patankar S V 1980 *Numerical heat transfer and fluid flow* (Hemisphere)
[14] Sung H J, Jang H C and Cho C H 1990 *Proc. Intern. Symp. on Eng. Turb. Model. Exp.* 33-42
[15] Gosman A D and Ioannides E 1983 *Journal of Energy* **7** 482-490
[16] Crowe C T, Sharma M P and Stock D E 1977 *J. Fluids Eng.* **99** 325-332
[17] Sommerfeld M, Qiu H H, Ruger M, Kohnen G. and Muler D 1993 *Proc. 2nd Int. Symp. on Eng. Turb. Model. Exp.* 935-945
[18] Sommerfeld M and Qiu H H 1998 *Int. J. Heat Fluid Flow* **19** 10-22
[19] Chen X Q and Pereira J C F 1996 *Int. J. Heat Mass Transfer* **39** 441-454